The Integration Spectrum of Spatial Markets: Measuring Arbitrage Across Timescales*

Siddhartha S. Bora†
West Virginia University
siddhartha.bora@mail.wvu.edu

Alankrita Goswami‡
University of Manitoba
alankrita.goswami@umanitoba.ca

Abstract

Conventional measures of spatial market integration compress adjustment across economic horizons into a single statistic. We introduce the integration spectrum, a horizon-specific measure of transport-cost pass-through, and show that conventional scalar estimates can mask substantial heterogeneity in transport-cost pass-through across horizons even when pass-through is near one-for-one at long horizons. Using weekly corn price spreads between the Illinois interior and the Louisiana Gulf from 2000–2026, we find that conventional scalar regressions imply partial pass-through, while the horizon decomposition reveals a marked gradient: weak transmission at short horizons and near one-for-one parity at long horizons. An exact decomposition shows how the scalar coefficient aggregates these horizon-specific relationships. Low-frequency, gain-phase, and simulation diagnostics indicate that filtering, temporal displacement, and measurement error do not fully account for the pattern. Seemingly incomplete integration in scalar measures can therefore coexist with near one-for-one transport-cost pass-through at long horizons.

Keywords: spatial price dispersion, market integration, transportation costs, price transmission, agricultural commodities
JEL: Q13, Q11, C43, C32

*This manuscript is a preliminary working draft. The views expressed in this manuscript are those of the authors and do not necessarily reflect those of their institutions or funding organizations. All remaining errors are the authors' own. Please contact the authors for any questions.

†Siddhartha Bora's work was supported in part by USDA-NIFA Hatch project (Accession number 7005656).

‡Alankrita Goswami acknowledges financial support from Manitoba Crop Alliance for her work.

1 Introduction

Empirical research across a wide range of markets documents that spatial price differentials between separated trading centers persistently exceed contemporaneous transportation costs over extended periods (Baulch, 1997; Fackler & Tastan, 2008; Stephens et al., 2012), and such departures are often interpreted as evidence of incomplete market integration (Barrett, 1996; Barrett & Li, 2002; Fackler & Goodwin, 2001). How that integration is measured, however, is itself the question. Conventional assessments compress adjustment that occurs at different economic horizons into a single scalar coefficient or long-run statistic (McNew & Fackler, 1997; Stigler & Sherwin, 1985; von Cramon-Taubadel & Goodwin, 2021), and that aggregation can make a market appear only partially integrated even when transport-cost pass-through approaches one-for-one at sufficiently long horizons (Goodwin & Piggott, 2001; Nigatu & Adjemian, 2020; Sephton, 2003). The aggregation matters because spatial arbitrage is inherently dynamic: when storage and transportation take time, temporary departures from contemporaneous transport-cost parity can arise even under competitive arbitrage (Coleman, 2009), as information can move across markets almost immediately while grain, inventories, and transportation capacity adjust more slowly. This study therefore asks whether spatial market integration can be measured as a process unfolding across economically meaningful timescales, rather than as a single long-run outcome.

Our question sits at the intersection of several literatures. Spatial equilibrium theory describes when prices in linked markets differ by no more than transfer costs (Enke, 1951; Samuelson, 1952; Takayama & Judge, 1971). The law-of-one-price tradition tests that prediction by relating spatial price transmission to transport costs (Goodwin & Schroeder, 1991; Goodwin et al., 1990; Ravallion, 1986). A related line of work uses cointegration and error-correction methods to characterize the long-run linkage between separated prices (Engle & Granger, 1987; Goodwin & Schroeder, 1991; McNew & Fackler, 1997), and threshold and parity-bound models add transaction costs that create bands of inaction around the law of one price (Balke & Fomby, 1997; Barrett, 1996; Barrett & Li, 2002; Goodwin & Piggott, 2001). The theory of storage, in turn, explains why a single market's price need not equal expected future prices, since storage and slow transport both allow temporary deviations from strict parity (Brennan, 1958; Coleman, 2009; Working, 1948, 1949); delivery lags and expectations complicate contemporaneous inference further (Lence et al., 2018). Closely related to our approach, frequency-domain methods have been applied directly to agricultural price integration (Nigatu & Adjemian, 2020). What these literatures share is a focus on whether markets are linked, whether deviations from

parity revert, and whether linkage varies across regimes. To our knowledge, none treats the horizon at which transport-cost discipline appears as the object of measurement.

We study this question using weekly U.S. corn price spreads between the Illinois interior and the Louisiana Gulf export market from 2000 through 2026. Prices are cash quotes from the U.S. Department of Agriculture's Agricultural Marketing Service (AMS), and transport costs are barge freight rates from USDA AgTransport. Because the main arbitrage cost is observed directly rather than inferred, the corridor is well-suited to testing transport-cost parity; a broader panel of local corn basis series provides corroborating evidence of cross-market comovement. We split both the price spread and the transport cost into four horizons fixed in advance: transient, storage, seasonal, and trend. We then estimate contemporaneous transport-cost pass-through within each. We call the resulting profile the *integration spectrum*: it describes spatial integration across adjustment horizons rather than collapsing it into a single number.

This study makes four contributions. First, we introduce the integration spectrum as a new measurement object: horizon-specific, contemporaneously aligned transport-cost pass-through. Second, we show that this object nests the conventional scalar coefficient rather than contradicting it. Under orthogonal bands, the single pass-through estimate is a transportation-cost-variance-weighted average of the horizon-specific coefficients; with finite filters, an additional cross-band covariance component remains. We call this component the *finite-filter covariance wedge*; it captures co-movement between transport cost and the spread across horizons. This is a spatial, transport-cost-parity object, distinct from the storage rate "wedge" driving the delivery-period futures–cash nonconvergence literature (Adjemian et al., 2013; Garcia et al., 2015; Goswami et al., 2022). In the Illinois–Gulf corridor, this component is modest and concentrated almost entirely in adjacent horizons. Third, we document an economic finding about the timing of arbitrage. Contemporaneous transport-cost pass-through is weak at transient horizons and close to one-for-one at the trend, and this holds for both the barge specification and the minimum-of-barge-or-rail robustness. At the same time, short-run cross-market basis comovement is strong even where transient transport-cost pass-through is weak. This indicates that common information can transmit rapidly across markets before physical arbitrage has imposed transport-cost parity. Fourth, we validate this gradient against mechanical alternatives. A filter-free low-frequency projection, following Müller and Watson (2018), does not reject one-for-one pass-through at the trend under either cost definition. The estimated gain approaches unity as the horizon lengthens, and the low-frequency phase implies a lag of only about two weeks, too short for delay alone to produce the gradi-

ent. In simulations, neither timing frictions nor measurement error on its own reproduces the observed spectrum, and the transient-below-trend ordering survives every robustness check.

Taken together, these results recast what a scalar regression reports as incomplete integration. Partial scalar pass-through can coexist with weak short-horizon transport-cost discipline and near one-for-one long-horizon pass-through. Seeing this requires measuring integration horizon by horizon rather than as a single coefficient and distinguishing rapid cross-market comovement from the horizon at which transport-cost discipline emerges. The reading is not specific to corn: wherever a spatial price spread can be paired with an observed transfer cost, the same horizon-by-horizon decomposition applies, and other corridors and commodities may exhibit integration gradients of their own.

The remainder of the paper proceeds as follows. Section 2 develops the conceptual framework and measurement object. Section 3 describes the corn data and the Illinois–Gulf corridor. Section 4 presents the empirical framework, estimation strategy, and validation exercises. Section 5 reports the integration spectrum, timing diagnostics, robustness, and limitations. Section 6 concludes.

2 Theoretical Framework

2.1 Storage and spatial arbitrage

A rational expectations framework that combines storage and spatial arbitrage implies that local spot prices are determined by decisions made by forward-looking, risk-neutral arbitrageurs. These traders allocate commodity quantities for current consumption using inventories carried from the previous period (Deaton & Laroque, 1992; Scheinkman & Schechtman, 1983; Williams & Wright, 1991). Each location has a separate inverse-demand function:

$$P_{m,t} = D_m(Q_{m,t}, \varepsilon_{m,t}), \quad D'_m < 0, \tag{1}$$

where m denotes origin (o) or destination (d), $Q_{m,t}$ is the quantity released for current use at the location, and $\varepsilon_{m,t}$ captures the local net-demand shocks.

The theory of storage emphasizes that carrying inventory from one period to the next produces both costs and benefits (Brennan, 1958; Kaldor, 1939; Telser, 1958; Working, 1948, 1949). The total cost of storing inventories $I_{m,t}$ at a location for competitive storers is:

$$K_m(I_{m,t}) = \delta_{m,t} - \gamma_m(I_{m,t}), \tag{2}$$

where $\delta_{m,t}$ denotes the physical warehousing cost and the convenience yield $\gamma_m(I_{m,t})$ represents the implied benefit storers derive from possessing inventories. Given the contemporaneous cash price $P_{m,t}$ determined in the spot market, the expected discounted profit from carrying inventory $I^i_{m,t}$ from period t to period $t+h$ for a competitive storer i at location m is:

$$E_t[\pi^i_{m,t+h}] = [\phi_{t,h}E_t(P_{m,t+h}) - P_{m,t} - K_m(I_{m,t})]\, I^i_{m,t}, \tag{3}$$

where $\phi_{t,h}E_t(P_{m,t+h})$ is the discounted expected value when the unit is sold in the $t+h$ period. Under the storage optimality conditions, there is no unexploited marginal profit opportunity in competitive equilibrium:

$$[\phi_{t,h}E_t(P_{m,t+h}) - P_{m,t} - K_m(I_{m,t})]\, I^i_{m,t} = 0, \tag{4a}$$

$$\implies \phi_{t,h}E_t(P_{m,t+h}) = P_{m,t} + K_m(I_{m,t}). \tag{4b}$$

Equations (1) – (4) establish the role of storage in facilitating the intertemporal allocation of inventories, thereby linking current prices to expected future prices.

While storage creates opportunities for intertemporal arbitrage, moving grains across locations enables a second mechanism: spatial arbitrage. Let P^d_t and P^o_t denote contemporaneous prices at an origin and destination, respectively. The spatial price spread is observed as:

$$S_t = P^d_t - P^o_t, \tag{5}$$

Williams and Wright (1991) assume instantaneous transportation from the origin to the destination, with an observed transportation cost C_t and additional transfer costs A_t not contained in the observed transportation charges. Under the condition of instantaneous shipment, the marginal spatial arbitrage return from trading across locations is:

$$R^T_t(0) = P^d_t - P^o_t - C_t - A_t, \tag{6}$$

Competitive spatial arbitrage requires (Enke, 1951; Samuelson, 1952):

$$R^T_t(0) \leq 0, \quad T^{od}_t \geq 0, \quad \text{and} \quad T^{od}_t \times R^T_t(0) = 0, \tag{7}$$

where T^{od}_t is the shipment quantity from location o to d. Consequently, if trade occurs, then the spatial price spread equals the total cost of moving the commodity:

$$S_t = C_t + A_t, \tag{8}$$

If trade does not occur, the price spread may be smaller than the total cost of transfer:

$$S_t \leq C_t + A_t, \tag{9}$$

Barrett and Li (2002) emphasize that market integration, competitive equilibrium, and observed trade are related but not equivalent. That implies equation (8) need not hold as an exact equality in every period, nor does the absence of trade necessarily suggest market segmentation. Our framework builds on their work, allowing us to account for commodity tradability across spatially distinct markets even when spatial equilibrium conditions may or may not be binding. Next, we take inspiration from Coleman (2009) and relax the assumption of instantaneous trade. Therefore, when the shipment takes τ periods to reach the destination d from the origin o, the trader then compares the current origin price and transportation costs with the expected destination price when the shipment arrives:

$$R_t^T(\tau) = \phi_{t,\tau} E_t(P_{t+\tau}^d) - P_t^o - C_t - A_t, \tag{10}$$

where $\phi_{t,\tau}$ is the discount factor that captures both the financing costs and the deterioration rate associated with the commodity over the period of delay. The slow-transportation arbitrage conditions are:

$$R_t^T(\tau) \leq 0, \quad T_t \geq 0, \quad \text{and} \quad T_t \times R_t^T(\tau) = 0, \tag{11}$$

Following (11), if a positive marginal shipment is observed, then the forward-arrival arbitrage condition is:

$$\phi_{t,\tau} E_t(P_{t+\tau}^d) = P_t^o + C_t + A_t, \tag{12}$$

At the same time, if the inventories at the destination are observed as positive, then under the storage optimality conditions shown in (4) (with $h = \tau$):

$$\phi_{t,\tau} E_t(P_{t+\tau}^d) = P_t^d + K^d(I_t^d), \tag{13}$$

Therefore, even when considering a scenario of delayed (but positive) shipment and positive inventories at the destination, equating equations (12) and (13) redefines the spatial price spread to be:

$$S_t = C_t + A_t - K^d(I_t^d), \tag{14}$$

This way, the contemporaneous spread need not equal transportation cost alone, but also

reflects other transfer costs and the total cost of carrying inventories at the destination. If the destination inventories are exhausted, the storage equality becomes an inequality (conditional on positive shipment):

$$S_t \geq C_t + A_t - K^d(0), \qquad \text{if } I_t^d = 0 \text{ and } T_t > 0, \tag{15}$$

The equation (15) follows the mechanism described by Coleman (2009). It emphasizes that when destination inventories are low and transportation is slow, the current destination spot price, and therefore the spatial price spread, can rise sharply even when the market is in competitive equilibrium.

Our theoretical framework draws on Coleman's slow-transportation condition to explain why the contemporaneous spatial price spread may differ from the observed transportation cost. Assuming positive destination inventories, substituting the value of $\phi_{t,\tau} E_t(P_{t+\tau}^d)$ from equation (13) back into equation (10) and rearranging gives:

$$S_t = C_t + \Omega_t(\tau), \qquad \text{if } I_t^d \geq 0 \tag{16}$$

where

$$\Omega_t(\tau) = R_t^T(\tau) + A_t - K^d(I_t^d). \tag{17}$$

This $\Omega_t(\tau)$ collects the net return from trade across geographic locations, other transfer costs, and destination inventory carrying costs.

2.2 The integration spectrum

Equations (16)–(17) decompose the contemporaneous spatial spread into the observed transportation cost and an unobserved component, $\Omega_t(\tau)$, that captures the remaining forces affecting the spread, including storage conditions, shipment delays, and other transfer costs. We do not estimate this relationship structurally. $\Omega_t(\tau)$ is unobserved, and the shipment delay τ is itself unobserved and may vary across time. Instead, we measure the observable contemporaneous relationship between the spatial spread and transportation cost, allowing that relationship to differ across economically meaningful horizons.

We pre-specify four horizon bands, namely, Transient (TR): < 8 weeks, Storage (ST): $8 - 32$ weeks, Seasonal (SE): $32 - 64$ weeks, and Long-term (LT): > 64 weeks. These labels describe the horizons over which variation in the spread and transportation cost is decomposed, and they do not imply structural identification of a distinct underlying mechanism at each horizon.

Definition 1 (Band-specific in-phase pass-through)**.** For band $j \in \{\mathrm{TR}, \mathrm{ST}, \mathrm{SE}, \mathrm{LT}\}$, let $S_t^{(j)}$ and $C_t^{(j)}$ denote the corresponding band-specific components of the spatial spread and observed transportation cost. We estimate

$$S_t^{(j)} = \alpha_j + \beta_j C_t^{(j)} + u_t^{(j)}, \qquad j \in \{\mathrm{TR}, \mathrm{ST}, \mathrm{SE}, \mathrm{LT}\}. \tag{18}$$

The vector

$$\mathcal{I} = (\beta_{\mathrm{TR}}, \beta_{\mathrm{ST}}, \beta_{\mathrm{SE}}, \beta_{\mathrm{LT}}) \tag{19}$$

is the *integration spectrum*.

For centered band components, equations (16)–(17) imply

$$\beta_j = 1 + \frac{\mathrm{Cov}\left(C_t^{(j)}, \Omega_t^{(j)}\right)}{\mathrm{Var}\left(C_t^{(j)}\right)}, \tag{20}$$

where $\Omega_t^{(j)}$ denotes the band-specific component of $\Omega_t(\tau)$. Equation (20) provides an accounting interpretation of the band coefficient. The coefficient β_j measures the contemporaneously aligned, or *in-phase*, response of the spatial spread to variation in observed transportation cost within band j. It does not separately identify storage, shipment delays, expectations, navigation conditions, or other transfer-cost components.

A value of β_j different from one therefore reflects covariance between transportation costs and the other components of the spatial spread at that horizon. Positive covariance raises β_j above one, while negative covariance lowers it below one. If the band-specific transportation cost and $\Omega_t^{(j)}$ are uncorrelated, then $\beta_j = 1$, even though $\Omega_t^{(j)}$ itself need not be zero. Thus, one-for-one pass-through is a statement about the response of the spread to transportation-cost variation, not equality between the levels of the spread and observed transportation cost. Because the regression is contemporaneously aligned, a coefficient below one need not imply proportionally weak structural transmission. It may reflect a smaller response magnitude, temporal displacement between transportation-cost changes and price adjustment, or both. We therefore complement the integration spectrum with gain and phase diagnostics that distinguish these possibilities.

If spatial arbitrage unfolds across multiple adjustment horizons, a single scalar summary necessarily combines economically distinct price–transportation-cost relationships and may therefore conceal horizon heterogeneity. The integration spectrum makes this heterogeneity, rather than its scalar average, the object of measurement. This relationship can be stated precisely. Suppose that the transportation-cost bands are mutually orthog-

onal and that cross-band spread–transportation-cost covariances are zero. Then the conventional scalar OLS coefficient that ignores horizon structure is exactly a transportation-cost-variance-weighted average of the band-specific coefficients.

Proposition 1 (Band decomposition of the conventional estimate)**.** *If the transportation-cost bands are mutually orthogonal and* $\mathrm{Cov}(S_t^{(j)}, C_t^{(k)}) = 0$ *for* $j \neq k$*, then the conventional scalar OLS coefficient satisfies*

$$\beta^{\mathrm{OLS}} = \sum_j w_j \beta_j, \qquad w_j = \frac{\mathrm{Var}\left(C_t^{(j)}\right)}{\mathrm{Var}(C_t)}, \qquad \sum_j w_j = 1, \tag{21}$$

where $j \in \{\mathrm{TR}, \mathrm{ST}, \mathrm{SE}, \mathrm{LT}\}$.

This result connects the integration spectrum to the logic of band spectrum regression (Engle, 1974; Granger, 1966). The conventional scalar estimate is therefore not an alternative to the integration spectrum, but a particular transportation-cost-variance-weighted aggregation of it. With finite filters, however, the band components need not be exactly orthogonal. In that case, cross-band covariance terms remain, and the exact finite-sample decomposition contains an additional *finite-filter covariance wedge* beyond the weighted within-band component in equation (21).

3 Data and Descriptive Statistics

3.1 Prices and the Illinois–Gulf corridor

We use weekly U.S. corn cash prices from the USDA Agricultural Marketing Service (U.S. Department of Agriculture, Agricultural Marketing Service, 2026b, 2026c), to construct local basis series. For market i,

$$b_i(t) = \mathrm{cash}_i(t) - F(t), \tag{22}$$

where $\mathrm{cash}_i(t)$ is the local cash price and $F(t)$ is the common corn futures price in week t. The futures roll convention is fixed in advance and applied uniformly across locations. We use the broader panel of local basis series as a descriptive measure of cross-market comovement after expressing local cash prices relative to a common futures benchmark. Because the same futures price enters each basis series, part of the observed basis comovement may reflect their common futures-price component rather than direct comovement

among local cash prices. We therefore treat the basis correlations as descriptive evidence of broad cross-market comovement. The direct spread–transport-cost analysis, by contrast, focuses on the Illinois–Louisiana Gulf corridor, where the spread is itself a difference of two cash prices that removes the common futures leg exactly, and where a route-specific transportation charge is observed.

The Illinois–Gulf corridor links a major U.S. corn-producing region to the primary Gulf export gateway along a route whose barge freight cost is directly observed (Birge et al., 2022; Miljkovic et al., 2000). Our empirical application relates weekly Illinois interior corn prices to weekly cash prices at the Louisiana Gulf export market, with the spatial spread defined as

$$S_t = P_t^G - P_t^{IL}, \tag{23}$$

where P_t^G is the Gulf cash price and P_t^{IL} is the Illinois cash price. Observed transportation costs come from USDA AgTransport (U.S. Department of Agriculture, Agricultural Marketing Service, 2026a, 2026d, 2026e) and are expressed in dollars per bushel so that the transportation charge and spatial spread share common units. Barge freight is the baseline and headline specification because it directly prices the principal waterborne route from the interior grain system to the Gulf. Because rail is an alternative mode during parts of the sample, we also construct a robustness series equal to the lower of the observed barge and rail costs. This specification asks whether the horizon pattern is sensitive to allowing the cheaper observed mode to discipline the spread; barge freight remains the baseline corridor measure.

Interpreting the band coefficients requires the spread and transportation cost to be commensurate, so we express both in dollars per bushel. We verify the freight conversion against the underlying tariff and rate schedule and fix the origin, destination, route, weekly alignment, and missing-data conventions before estimation. Because weekly price quotes and freight observations need not refer to the same instant, we treat any resulting timing mismatch as temporal displacement and address it through the diagnostics in Section 4.3.

3.2 Descriptive statistics

Table 1 summarizes the principal variables. The Illinois–Gulf spread is observed for 1,344 weeks and averages approximately \$0.69 per bushel. The minimum observed transport cost, $\min(\text{barge}, \text{rail})$ in each week, averages approximately \$0.58 per bushel over its coverage sample, while barge freight, the baseline single-mode series, averages approximately \$0.57 per bushel. Rail is higher on average and is the cheaper observed mode in only 49

weeks.

Table 1: Summary statistics, Illinois–Gulf corridor (weekly, $/bu).

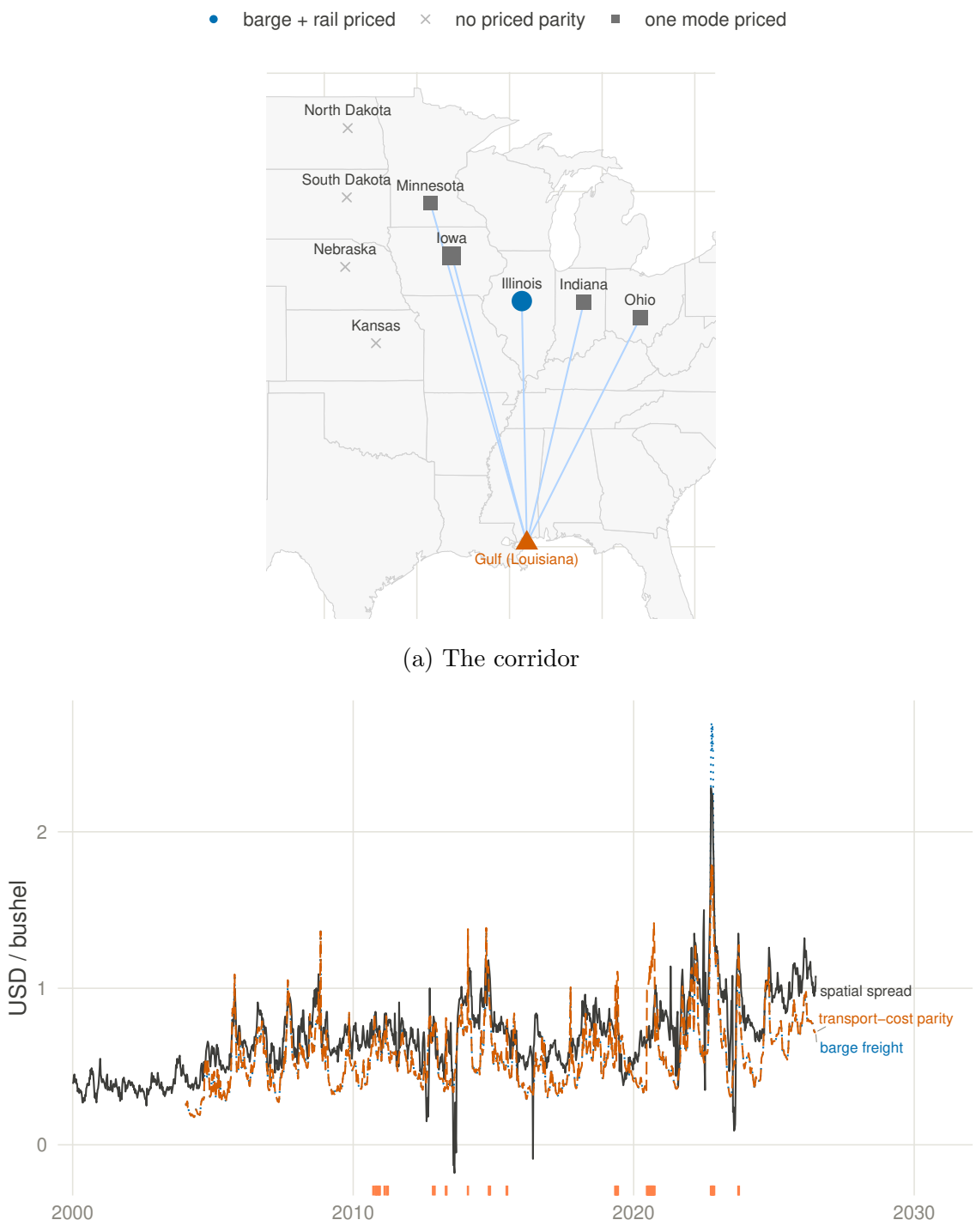
variable	N	mean	SD	min	median	max
Spatial spread (Gulf - Illinois, USD/bu)	1344	0.685	0.254	-0.18	0.68	2.28
Transport-cost parity (USD/bu)	1141	0.578	0.225	0.177	0.54	1.794
Barge freight (USD/bu)	1116	0.572	0.243	0.177	0.533	2.696
Rail freight (USD/bu)	761	1.027	0.252	0.571	0.998	2.171
Illinois basis (USD/bu)	989	-0.156	0.257	-1.31	-0.206	1.474
Gulf basis (USD/bu)	980	0.609	0.29	-0.56	0.552	2.444

Notes: Each variable is summarised over its own coverage sample, so the ratio of the spread and transport-cost means shown here (about 1.19) differs from the corresponding ratio on the common priced/aligned sample used in estimation (mean ratio ≈ 1.3; Section 5.1).

On the common priced and aligned sample used in estimation, the average spread is approximately 1.3 times the observed transportation cost. Figure 1 shows the corridor and the principal series. Panel (a) places the Illinois origin and Gulf destination within the broader set of corn-market locations represented in the price data. Panel (b) plots the Illinois–Gulf spatial spread together with the minimum observed transport cost and barge freight from 2000 through 2026. The spread and transport-cost series share broad low-frequency movements but exhibit sizable short-run departures, motivating the horizon decomposition developed below.

The ticks below Figure 1b mark the 49 weeks in which rail is the cheaper observed mode, concentrated around 2010 and 2019–2022. These weeks are distinct from the larger minimum-of-barge-or-rail estimation sample, which uses the cheaper observed mode whenever the relevant price and freight data are jointly available and therefore contains 1,174 weeks, compared with 859 for the barge specification (Table 2). Transportation-cost variation is also distributed unevenly across horizons, and these variance shares determine the weights with which the band-specific coefficients enter the scalar aggregation in Proposition 1. We report them alongside the integration spectrum in Figure 2.

We situate the integration spectrum against the traditional time-series measures of spatial linkage familiar from the spatial-price literature, such as cointegration, error-correction adjustment, and impulse-response summaries. Their role here is comparative: they characterize broad long-run linkage and adjustment, whereas the integration spectrum asks how the observed spread–transport-cost relationship is distributed across horizons. Section 5.4 contrasts the two conceptually and illustrates the distinction with a pair of simulated market systems (Appendix A).



(a) The corridor

(b) Spread and transport cost

Figure 1: The Illinois–Gulf corridor. (a) origins (point size, priced weeks) and the Gulf destination; (b) weekly spatial spread, minimum observed transport cost (the lower of barge and rail), and barge freight, 2000–2026 (ticks below the panel mark rail-marginal weeks).

4 Empirical Framework

4.1 Estimation strategy

We apply the same pre-specified finite filter bank to the spatial spread S_t and observed transportation cost C_t (Baxter & King, 1999; Christiano & Fitzgerald, 2003; Percival & Walden, 2000; Vetterli & Herley, 1992). The decomposition produces the four components defined in Section 2 and preserves the economically chosen horizon boundaries rather than selecting bands to maximize fit. For each band j, we estimate equation (18) and report the in-phase coefficient $\hat{\beta}_j$ with moving-block-bootstrap confidence intervals. The estimand is explicitly reduced-form: β_j is the linear projection of the band-j spatial spread on the band-j observed transportation cost, and we use "pass-through" throughout as shorthand for this contemporaneously aligned association rather than for a causal response to an exogenous freight-cost shock. Because observed freight rates are not exogenous, β_j generally reflects covariance between transportation cost and the other determinants of the spread within band j, as equation (20) makes explicit. The bootstrap preserves local serial dependence in the filtered series (Künsch, 1989; Politis & Romano, 1994), which is important because each band component is mechanically persistent over its associated horizon.

The primary summary of horizon heterogeneity is the transient-to-trend gap,

$$\Delta_{LT} = \beta_{\mathrm{LT}} - \beta_{\mathrm{TR}}. \tag{24}$$

We also test the flat-spectrum null

$$H_0 : \ \beta_{\mathrm{TR}} = \beta_{\mathrm{ST}} = \beta_{\mathrm{SE}} = \beta_{\mathrm{LT}}. \tag{25}$$

Because the conventional asymptotic Wald reference distribution is anti-conservative for the available sample size, the headline test is calibrated via simulation. Under the flat-spectrum Monte Carlo described below, the nominal 5 percent asymptotic test rejects approximately 28.5 percent of the time. We therefore report simulation-calibrated critical values and the corresponding calibrated rejection rather than treating the raw asymptotic p-value as decisive.

With finite filters, exact orthogonality is an empirical rather than automatic property. Accordingly, we use the exact covariance accounting in the sample. Writing $C_t = \sum_j C_t^{(j)}$ and $S_t = \sum_j S_t^{(j)}$, the scalar numerator can be decomposed into within-band and cross-band covariances (Whitcher et al., 2000). The within-band component is $\sum_j w_j \hat{\beta}_j$, while

the remaining cross-band terms form the finite-filter covariance wedge. This accounting allows us to quantify rather than assume away departures from the orthogonal-band identity in Proposition 1.

4.2 Monte Carlo validation

We use several simulation exercises, each for a distinct purpose. The first is a known-spectrum recovery design. We impose a data-generating process with a known horizon-specific transportation-cost response and pass the simulated series through the same finite-filter and estimation procedure used in the empirical analysis. The exercise asks whether the estimator can recover a deliberately non-flat spectrum when the truth is known. In the design reported in Appendix Figure A.1, the maximum absolute difference between the estimated and true band coefficients is 0.008, providing a direct check on recovery under the implemented decomposition.

A second exercise isolates temporal displacement. Holding the true gain flat and varying the response lag, it shows how much apparent band heterogeneity a contemporaneously aligned regression can display when transportation-cost changes reach the spatial spread with a delay (Figure 5a). The flat-spectrum Wald test is calibrated separately, under its own null: a flat true spectrum in which every band has the same contemporaneously aligned coefficient. We calibrate because the asymptotic reference distribution is anti-conservative at this sample length; under the flat-spectrum null the empirical size of the nominal 5 percent asymptotic test is 0.285, motivating the simulation-calibrated critical values reported in Table 2.

The simulation exercises serve different purposes. Known-spectrum recovery validates the implemented estimator against a known truth; the phase-displacement design illustrates what timing alone can generate; and the flat-spectrum null supplies the reference distribution used for inference on horizon heterogeneity. The separate cost-noise exercise in Section 5 is a stress test for an alternative measurement explanation rather than an additional source of identification. Appendix Table A.1 provides a complementary illustration. Two simulated market systems have very similar conventional long-run summaries but sharply different transient-band coherence. The exercise is not used as identification for the Illinois–Gulf estimates; rather, it demonstrates the measurement point that familiar long-run or univariate summaries can be nearly identical even when short-horizon transmission differs substantially.

4.3 Low-frequency benchmark and timing diagnostics

Filter-free low-frequency benchmark. The filtered trend coefficient is not the sole basis for the long-horizon result. We therefore estimate a low-frequency projection following Müller and Watson (2008, 2018). The procedure projects the spatial spread and observed transportation cost onto a small number of low-frequency components and conducts inference on their low-frequency covariability without relying on the wavelet/filter trend component used to construct the integration spectrum.

This benchmark asks whether the low-frequency relationship between the spatial spread and transportation cost is consistent with a unit slope under an inference procedure designed for persistent time series. Agreement between the low-frequency projection and the filtered trend coefficient also reduces the possibility that the long-horizon result is an artifact of the particular finite filter used in the main decomposition. We therefore treat the Müller–Watson projection as an independent low-frequency benchmark and the filtered trend coefficient as the corresponding component of the integration spectrum.

Gain, phase, and lead–lag diagnostics. The band coefficient β_j is an in-phase quantity. A low contemporaneous coefficient can arise because the spatial spread is only weakly aligned with transportation-cost variation, because the relationship is temporally displaced, or because both features are present. To distinguish response magnitude from timing, we estimate the spread–transport-cost transfer function

$$H(\omega) = \frac{f_{SC}(\omega)}{f_C(\omega)}, \tag{26}$$

where $f_{SC}(\omega)$ is the cross-spectrum between the spatial spread and transportation cost, and $f_C(\omega)$ is the transportation-cost spectrum. We summarize the frequency-domain relationship over the four horizon bands using the gain $|H(\omega)|$ and phase $\arg H(\omega)$ of $H(\omega)$, together with spread–cost coherence (Granger & Hatanaka, 1964; Priestley, 1981).

Gain describes the magnitude of the frequency-specific spread–cost relationship, while phase describes its temporal displacement. This distinction is important because a small contemporaneous β_j need not imply a proportionally weak frequency-specific relationship when spread and transportation-cost variation are temporally displaced. We therefore also estimate compact lead–lag regressions to assess whether allowing temporal displacement between transportation costs and the spread materially changes the short-horizon relationship.

These diagnostics do not replace the integration-spectrum estimates and are not in-

terpreted as structural identification of freight-cost shocks. Their purpose is to clarify the reduced-form meaning of the in-phase coefficients and, in particular, to assess whether the transient-to-trend gradient can be explained primarily by timing. As shown in Section 5, the response gain itself rises substantially with horizon, while the low-frequency phase corresponds to only about a two-week lag. The combined evidence therefore addresses two distinct concerns: whether the trend result depends on the filtering procedure and whether the weak transient coefficient is primarily a consequence of temporal displacement.

4.4 Measurement error

Measurement error affects the interpretation of the integration spectrum differently depending on whether it enters the spatial spread or the observed transportation cost. We therefore distinguish the two channels explicitly. Classical measurement error in the spatial spread is left-hand-side noise. Suppose

$$S_t^{\text{obs}} = S_t^* + \eta_t, \tag{27}$$

where η_t is classical relative to observed transportation cost. Such error increases residual variance and can reduce precision or lower R^2, but it does not mechanically attenuate the estimated pass-through coefficient. Measurement error in cash prices can therefore contribute to differences in goodness of fit across horizons without, by itself, generating the transient-to-trend slope gradient.

Measurement error in observed transportation cost is different because it enters the right-hand side of the band regression. If

$$C_t^{\text{obs}} = C_t^* + \nu_t, \tag{28}$$

with classical ν_t, the estimated relationship between the spatial spread and transportation cost is attenuated toward zero (Fuller, 1987). Cost-side measurement error is therefore capable, in principle, of producing weak short-horizon in-phase pass-through if noise is large relative to the underlying transportation-cost signal.

We evaluate this possibility with a targeted simulation that adds progressively larger amounts of classical noise to an otherwise correctly measured transportation-cost series while holding true pass-through equal to one. The exercise is intended as a stress test rather than an estimate of the actual measurement-error variance. It asks how much

transportation-cost noise would be required to generate a transient coefficient as small as that observed in the data while leaving the trend relationship close to one.

Timing mismatch is conceptually distinct from classical measurement error. Differences in quote or settlement timing primarily alter the phase relationship between the spatial spread and transportation cost and are therefore addressed by the gain, phase, and lead–lag diagnostics in Section 4.3. Keeping the two channels separate prevents temporal displacement from being interpreted as classical attenuation.

5 Results and Discussion

5.1 The Illinois–Gulf integration spectrum

Figure 2 and Table 2 report the Illinois–Gulf integration spectrum: contemporaneously aligned transport-cost pass-through, estimated separately within each of the four horizon bands. The estimates rise steeply with horizon. For the baseline barge specification, the band coefficients are approximately (0.21, 0.62, 0.57, 0.89) across the transient, storage, seasonal, and trend bands. The minimum-of-barge-or-rail specification gives (0.12, 0.74, 0.58, 1.10) on its larger sample. Contemporaneous transport-cost pass-through is therefore weak at short horizons and approximately one-for-one at long horizons. The confidence intervals for both specifications include one at the trend, while their point estimates bracket parity from either side.

The economically meaningful contrast is the rise from the transient band to the trend, not the ordering of the intermediate bands. The seasonal coefficient is just below the storage coefficient, so the spectrum need not be monotone across all bands. A flat spectrum, in which pass-through does not vary with horizon, is nonetheless decisively rejected: the observed Wald statistic is 85.5, against a simulation-calibrated 5% critical value of 21.3 ($p < 0.001$). We use the calibrated reference distribution rather than the asymptotic test, which is anti-conservative at this sample length (Table 2). The primary summary of this heterogeneity is the transient-to-trend gap $\Delta_{LT} = \beta_{\mathrm{LT}} - \beta_{\mathrm{TR}}$: for the baseline barge specification it is 0.68, with a 95% moving-block-bootstrap interval of [0.46, 0.95] that excludes zero, and it is 0.98 under the minimum-cost specification.

Long-run pass-through. Because the trend-band estimate anchors the parity claim, we corroborate it with a filter-free benchmark. The Müller–Watson low-frequency projection is our primary long-run measure, and the wavelet trend-band coefficient corroborates

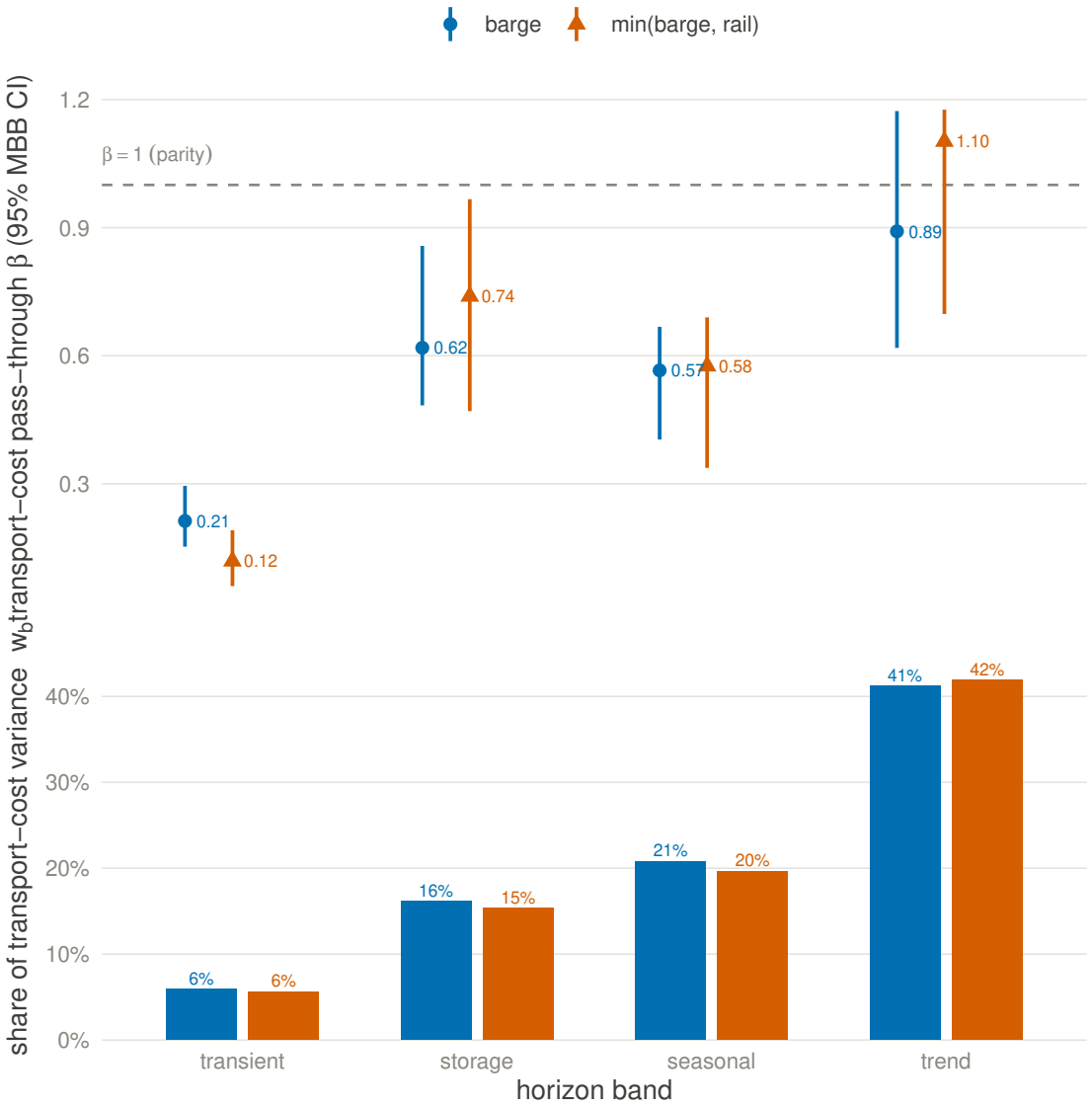


Figure 2: The Illinois–Gulf integration spectrum (top) and its transport-cost variance weights (bottom). Top: contemporaneously aligned pass-through β_b by horizon band with 95% moving-block bootstrap intervals; barge in blue circles, min(barge, rail) in vermillion triangles, each point labeled with its value, dashed line at $\beta = 1$. Bottom: $w_b = \mathrm{Var}(TC^{(b)})/\mathrm{Var}(TC)$, labelled in percent.

Table 2: Illinois–Gulf transport-cost pass-through by horizon band and cost definition.

cost def.	band	β_b	CI low	CI high	covers one	R^2	n
barge	transient	0.213	0.153	0.295	FALSE	0.038	859
barge	storage	0.618	0.484	0.857	FALSE	0.331	859
barge	seasonal	0.565	0.404	0.668	FALSE	0.597	859
barge	trend	0.891	0.618	1.173	TRUE	0.748	859
min(barge, rail)	transient	0.119	0.06	0.191	FALSE	0.013	1174
min(barge, rail)	storage	0.739	0.47	0.967	FALSE	0.436	1174
min(barge, rail)	seasonal	0.576	0.337	0.69	FALSE	0.646	1174
min(barge, rail)	trend	1.102	0.698	1.176	TRUE	0.822	1174

Notes: Columns, β_b, its 95% MBB interval, whether the interval covers one, R^2, and the effective sample n. Barge is barge freight; min(barge, rail) takes the cheaper of the two modes and estimates on a larger aligned sample ($n = 1174$ vs 859), the difference reflecting short-gap interpolation of the denser combined-mode series. The weeks in which rail is the marginal (cheaper) mode are a distinct, smaller set (49).
Flat-spectrum test: simulation-calibrated critical values 17.0 (10%), 21.3 (5%), 35.0 (1%); observed Wald statistic 85.5; calibrated $p < 0.001$.

Table 3: Filter-free long-run transport-cost pass-through: Müller–Watson low-frequency projection and the wavelet trend-band estimate, by cost definition.

method	cost def.	β	CI low	CI high	p ($\beta = 1$)	detail
Müller–Watson low-freq.	barge	0.894	0.677	1.111	0.324	q = 26
Müller–Watson low-freq.	min(barge, rail)	1.074	0.889	1.258	0.422	q = 36
Wavelet trend (LA8)	barge	0.891	0.618	1.173		214-wk block
Wavelet trend (LA8)	min(barge, rail)	1.102	0.698	1.176		293-wk block

Notes: Müller–Watson rows report β, a t-based 95% interval (df $= q - 1$), and the p-value against $\beta = 1$ (*detail* gives q, the number of low-frequency components); wavelet trend rows report β and its 95% MBB interval (*detail* gives the block length). Blank cells are not applicable to that row's method.

it. Neither rejects one-for-one pass-through at the trend for either cost definition: the projection gives $\beta = 0.89$ for barge and 1.07 for the minimum-cost series, with p-values of 0.32 and 0.42 against $\beta = 1$ (Table 3).

A trend coefficient near one means the spatial spread responds one-for-one to transport-cost variation at long horizons; it does not mean the spread equals observed cost. The spread nevertheless exceeds observed transportation cost by about 30% on average on the common priced sample (a mean ratio of roughly 1.3). This level difference is not governed by the slope coefficient and may reflect other transfer costs, including handling, quality, and contractual components that do not vary proportionally with freight.

Table 4: The scalar coefficient as an aggregation of the spectrum.

cost def.	β^{OLS}	$\sum_b \hat{w}_b \beta_b$	wedge	rel. wedge	$\sum_b \hat{w}_b$
barge	0.688	0.597	0.09	0.131	0.841
min(barge, rail)	0.791	0.695	0.096	0.122	0.825
known-spectrum sim	0.962	0.949	0.013	0.014	

Notes: β^{OLS}, the within-band weighted component, the wedge, and the weight sum, by cost definition; the last row is the known-spectrum simulation benchmark. The decomposition $\beta^{OLS} = \sum_b \hat{w}_b \beta_b +$ wedge holds exactly on the estimation sample. $\sum_b \hat{w}_b \approx 0.84$ (not one) because the finite-filter bands are not exactly orthogonal: their mutual cross-band transport-cost covariance enters $\mathrm{Var}(TC)$ in the denominator without being charged to any single band's variance share (Table 5 shows the source of this wedge).

Aggregation of the spectrum. The conventional scalar coefficient is an aggregation of this spectrum, not an alternative to it. On the estimation sample, the full-sample OLS estimate is $\hat{\beta}^{OLS} \approx 0.688$, and it decomposes exactly into a variance-weighted within-band component of about 0.597 and a cross-band covariance component of about 0.090 (Table 4). The band weights sum to about 0.84 rather than one because the finite-filter bands are not exactly orthogonal: their mutual cross-band transport-cost covariance enters the total variance in the denominator without being charged to any single band (Table 5).

A scalar coefficient near 0.69 is fully compatible with a market whose short-horizon in-phase pass-through is very weak and whose long-horizon pass-through is approximately one-for-one. Because the trend band carries about 42% of transport-cost variance (Figure 2, bottom), the scalar estimate is variance-weighted toward the trend, yet it still

Table 5: The finite-filter wedge is concentrated in adjacent band pairs.

band pair	adjacent	barge (%)	min-mode (%)
transient-storage	yes	11.26	7.364
transient-seasonal	no	0.028	0.022
transient-trend	no	0.001	0.001
storage-seasonal	yes	43.43	46.2
storage-trend	no	2.288	2.122
seasonal-trend	yes	42.99	44.3

Notes: Cross-band contribution to the wedge in Table 4, by band pair and cost definition. Adjacent pairs carry about 98% of the wedge and non-adjacent pairs about 2%, so it reflects filter-boundary sharing between neighboring bands rather than diffuse contamination.

understates long-run parity by averaging in the weaker short-horizon bands.

The band coefficients, however, do not identify the mechanisms underlying the horizon gradient. Either classical measurement error in observed cost or pure phase displacement between cost and spread could in principle flatten the transient coefficient while leaving the trend near one; as the robustness analysis below shows, neither, by itself, reproduces the full pattern, in particular the rise in response gain. The economic reading rests instead on the response gain rising toward one-for-one (Figure 4) and on the distributed-lag simulation (Table 6), not on the contemporaneous coefficients alone.

5.2 Timing, comovement, and the economics of adjustment

Comovement and coherence. Figure 3 sets two horizon profiles against each other: cross-market basis comovement and spread–cost coherence. The two run in opposite directions and cross at mid-horizon. Spread–cost coherence rises across the bands, from 0.12 at the transient band to 0.39, 0.66, and 0.74; cross-market basis comovement falls over the same range, from about 0.72 at the transient band to 0.31 at the trend.

This contrast is important for interpreting the horizon gradient. Comovement across markets is strong precisely where transient transport-cost pass-through is weak. The pattern is consistent with common information being reflected rapidly across markets even where transport-cost discipline remains weak at short horizons (Myers & Jayne, 2012; Stephens et al., 2012). The distinction matters because it separates concepts that are often conflated: statistical comovement, tradability, and competitive spatial equilibrium are not interchangeable (Barrett, 1996; Barrett & Li, 2002; McNew & Fackler, 1997).

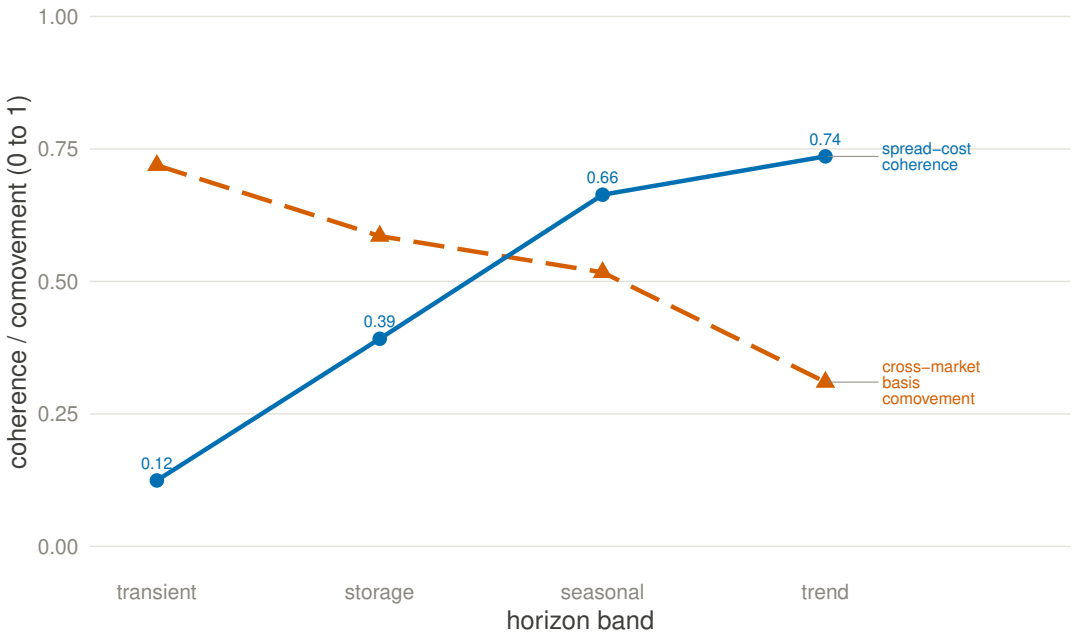


Figure 3: Cross-market basis comovement and spread–cost coherence by horizon band (both on a 0–1 scale). Each series is named at its right endpoint, coherence solid with circles, comovement dashed with triangles, and the coherence values are labeled.

The cross-market weekly-basis correlation matrix, a tight Corn Belt cluster with strong short-run comovement beyond the single corridor, is reported in Appendix A (Figure A.2).

Table 6: Simulation: delayed pass-through, all four bands (broad-band cost, six-week distributed lag).

band	contemporaneous β	cumulative β (distributed lag)
transient	0.286	0.847
storage	0.755	0.964
seasonal	1.006	1.05
trend	0.978	0.978

Notes: Contemporaneous and cumulative distributed-lag coefficients by band; the true structural (cumulative) pass-through is one in every band.

Gain and phase. The contemporaneous coefficient can understate the magnitude of the spread–cost relationship when the two series are temporally displaced, so we turn to the frequency response itself. The estimated gain rises with horizon toward one-for-one pass-through: from 0.39 at the transient band to 0.89 at the trend for barge, and from 0.35 to 1.04 for the minimum-cost series (Figure 4, top). The low-frequency phase corresponds

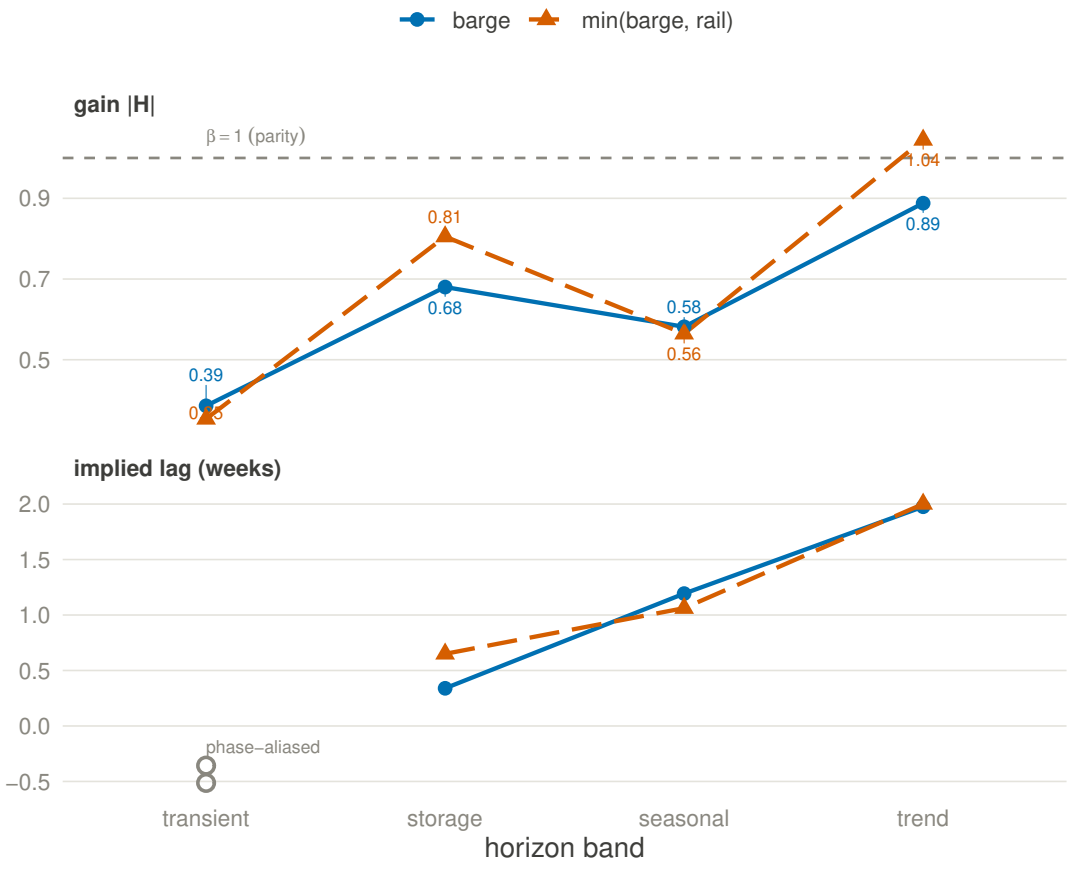


Figure 4: Transport-cost gain $|H|$ (top) and implied lag (bottom) by horizon band; barge solid with circles, min(barge, rail) dashed with triangles, gain values labelled. The transient-band lag is drawn as a hollow grey marker: it is phase-aliased and is not a delay estimate.

to a lag of only about two weeks. Adjusting for lead and lag therefore changes the timing interpretation but does not remove the increase in response magnitude. The rising gain, not the small trend lag, is the key evidence against pure temporal displacement as a complete explanation of the gradient.

The distributed-lag simulation in Table 6 illustrates this effect. When a common six-week distributed lag is imposed, and the true structural pass-through is one in every band, the contemporaneous coefficient is timing-attenuated at short horizons and approaches one as the horizon lengthens (0.29, 0.76, 1.01, 0.98): a six-week delay is large relative to the transient timescale but negligible at the trend. The cumulative distributed-lag sum, by contrast, recovers toward one in every band (0.85, 0.96, 1.05, 0.98). The small short-horizon contemporaneous coefficient should therefore be read as in-phase pass-through, not as the structural gain.

Interpretation. These results support a reduced-form interpretation rather than a structural one. Coleman (2009) provides a theoretical mechanism consistent with this interpretation: contemporaneous spot-price deviations need not imply failed arbitrage when shipment takes time, and inventories mediate adjustment. The integration spectrum does not, by itself, identify storage, congestion, information, or market power; its measured statement is narrower. Transport-cost discipline is strongly horizon dependent, with weak in-phase pass-through at short horizons and approximately one-for-one pass-through at long horizons.

5.3 Alternative explanations and robustness

We consider the leading alternative explanations for the gradient in turn, then summarize its robustness across specifications.

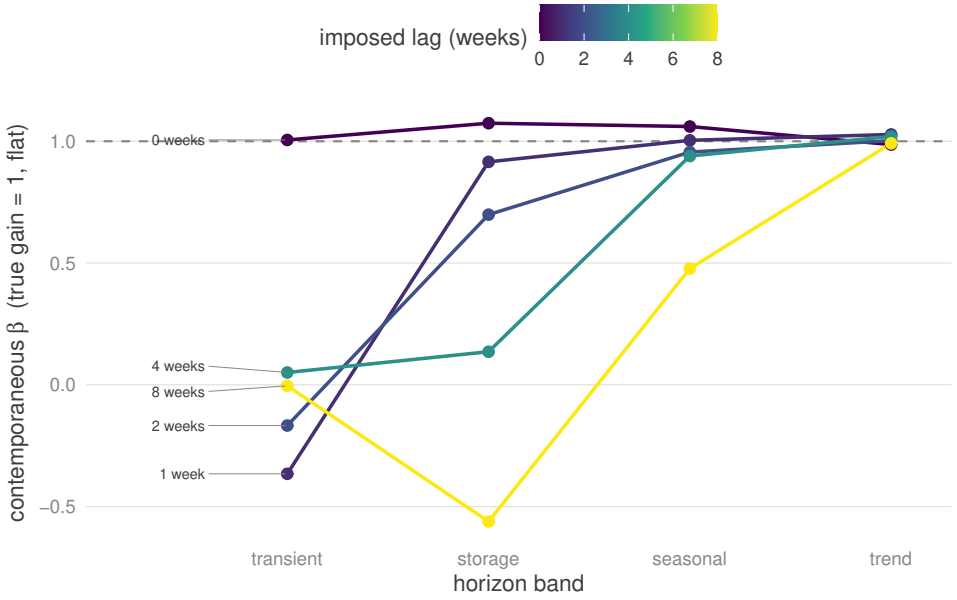
Finite-filter covariance. A natural concern is that imperfect filter separation could mechanically generate the horizon gradient. Two distinct pieces of evidence indicate that it does not account for the observed pattern. First, the known-spectrum recovery exercise is very accurate: passing a deliberately non-flat spectrum through the same decomposition returns the band coefficients with a maximum absolute error of 0.008, so finite-filter contamination is small when the truth is known. Second, the empirical cross-band covariance is not unexplained; it is the covariance wedge decomposed exactly in Table 4, and about 98% of it is concentrated in adjacent band pairs (Table 5). The wedge is about 13% of the scalar coefficient, larger than the 1.4% implied by the known-spectrum

benchmark, but its adjacent-band structure is consistent with its arising primarily from filter-boundary sharing rather than diffuse contamination.

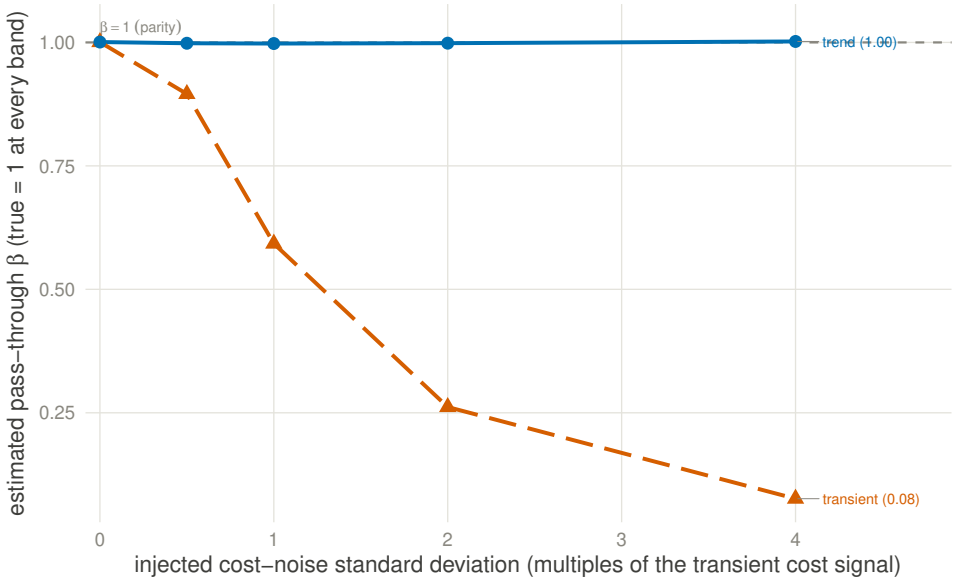
Flat gain with phase displacement. The flat-spectrum test establishes that the in-phase coefficients differ across horizons, but it does not establish that the underlying response gain differs; a pure timing displacement can generate a non-flat contemporaneous β profile even when the true gain is constant. Figure 5a shows this directly. Holding the true gain flat and imposing a pure L-week lag, the contemporaneous coefficient collapses at the transient band as L grows, reaching about zero by $L = 8$, while the trend coefficient stays near one (≈ 0.99). Pure timing can therefore generate a contemporaneous β gradient resembling the empirical one, and the β spectrum alone cannot distinguish such phase attenuation from a genuinely weaker short-horizon response. The empirical gain profile in Figure 4, however, provides evidence against pure phase displacement as a complete explanation: gain itself rises substantially with horizon, although the transient-band estimate is based on weak spread–cost coherence and should therefore be interpreted with caution.

Measurement error in prices and transport costs. Classical measurement error in the regressor deserves separate treatment because it attenuates slopes. Noise in the cash spread, however, is left-hand-side noise: it reduces precision and can steepen the R^2 profile across bands, but it cannot by itself attenuate the pass-through coefficient. The relevant channel is measurement error in observed transport cost. The unit-and-rate audit, however, limits the plausible magnitude of cost-side measurement error. High-frequency cost noise can mechanically produce transient attenuation: in the cost-noise simulation (Figure 5b) the transient slope falls from 1.00 to about 0.08, but only as the injected noise standard deviation reaches four times the transient cost signal, while the trend slope holds at parity (≈ 1.00). Attenuation of that magnitude requires an implausibly large noise-to-signal ratio, and, like pure timing, it leaves the rising empirical gain unexplained.

Settlement timing and asynchronicity. A related concern is that weekly quotes and freight settlements are not perfectly synchronous. We treat such mismatch as a phase contaminant rather than classical measurement error, so it is addressed by the same gain, phase, and lead–lag diagnostics reported above rather than folded into the cost-noise bound. Because those diagnostics show the response gain rising with horizon, within-week timing mismatch does not appear to provide a complete explanation for the increase.



(a) Timing alone (phase displacement)



(b) Measurement error alone

Figure 5: Mechanical alternatives to the integration spectrum. (a) Phase-displacement grid: band-wise contemporaneous β under a flat true gain with a pure L-week lag ($L = 0, 1, 2, 4, 8$, each line labeled with its lag at the transient end); timing collapses the transient band (to about zero by $L = 8$) but leaves the trend near one (≈ 0.99), so it cannot move the trend off parity. (b) Cost-noise attenuation: classical measurement error in observed cost collapses the transient slope (endpoints labeled) while the trend slope holds at parity. Neither mechanism, on its own, reproduces the observed spectrum, in which the response *gain* itself rises with horizon (Figure 4).

Robustness. Finally, we vary the specification along the dimensions that could plausibly drive the result: the band edges, the wavelet and filter choice, boundary trimming and the treatment of missing weeks, the barge-versus-minimum-cost definition, and the sample window (Table 7). The horizon gradient is not the artifact of any one of these choices. Across specifications the transient-to-trend gap ranges from about 0.68 to 1.10 and never changes sign, so the transient coefficient remains well below the trend coefficient throughout.

Table 7: Transient and trend pass-through and their gap across specifications.

dimension	variant	β_T	β_L	Δ_{LT}	$\beta_T < \beta_L$	n
reference	reference (LA8, min-mode)	0.119	1.102	0.983	TRUE	1174
band scheme	seasonal into storage	0.119	1.102	0.983	TRUE	1174
band scheme	strict trend (L7+)	0.119	1.184	1.065	TRUE	1174
wavelet	la16	0.118	1.101	0.983	TRUE	1174
wavelet	d4	0.131	1.105	0.974	TRUE	1174
wavelet	haar	0.177	1.116	0.94	TRUE	1174
transport cost	barge-only	0.213	0.891	0.678	TRUE	859
missing weeks	no interpolation	0.268	1.167	0.9	TRUE	188
missing weeks	max gap 8	0.119	1.102	0.983	TRUE	1174
sample window	recent 350 weeks	0.128	1.104	0.976	TRUE	350
interior-only	boundary-masked	0.116	1.102	0.986	TRUE	1132

Notes: Specifications span band edges, wavelet/filter, cost definition, missing-week handling, sample window, and boundary trimming; the final column flags whether the ordering $\beta_{\mathrm{TR}} < \beta_{\mathrm{LT}}$ holds.

5.4 Relationship with existing measures and limitations

Relationship with existing measures. The integration spectrum is complementary to existing measures of spatial linkage, not a correction of them. Cointegration and error-correction summaries characterize long-run linkage and the speed of adjustment (Engle & Granger, 1987; Johansen, 1988); threshold models describe regime-dependent transaction costs (Balke & Fomby, 1997; Goodwin & Piggott, 2001); coherence measures capture comovement (Nigatu & Adjemian, 2020). What they do not reveal is how the relationship between the spatial spread and observed transport cost varies across horizons, which is the quantity the spectrum measures. A complementary simulation in Appendix A makes the gap concrete: two market systems with nearly identical conventional long-run summaries can differ sharply in their short-horizon behavior (Table A.1).

Limitations. Several limitations bound these conclusions. The bands are pre-specified rather than estimated, and finite filters make their orthogonality approximate rather than exact. The strongest direct transport-cost evidence comes from a single corridor; the broader corn-market comovement evidence corroborates the picture but does not substitute for corridor-specific freight identification. Most important, the interpretation is reduced-form: the spectrum measures horizon dependence in transport-cost discipline, but it does not separately identify inventories, shipment timing, congestion, information, or market power.

6 Conclusions and Future Work

This paper asks whether the responsiveness of the spatial price spread to transport-cost variation differs across economically distinct horizons, thereby making the horizon-specific pattern of spatial market integration the object of measurement. To answer this question, we focus on the Illinois–Gulf corn transport corridor, which connects one of the major corn-producing regions to the Gulf export market, and for which a directly observed time series of route-relevant barge freight costs is matched with weekly origin and destination prices from 2000–2026. By design, the integration spectrum measures how the contemporaneously aligned relationship between the spatial price spread and observed transportation cost varies across different timescales. It estimates reduced-form transport-cost pass-through separately over four pre-specified bands: transient, storage, seasonal, and trend. These bands are motivated by the temporal windows over which one might expect inventory allocation decisions, seasonality, and physical transportation-related frictions to affect spatial prices. The resulting spectrum reveals substantial horizon-dependent heterogeneity that is concealed by a conventional scalar estimate. Pass-through is very weak below eight weeks, becomes economically substantial over the pre-specified 8–32 week storage horizon, and is statistically consistent with one-for-one responsiveness at the trend horizon. This strengthening of the spread–cost relationship at intermediate and longer horizons is consistent with mechanisms emphasized in the storage and spatial-arbitrage literature, in which inventory decisions and the time required for physical transportation allow spatial-price adjustment to unfold over time. Given that the current estimation does not yet incorporate direct measures of inventories and shipment timing, the band coefficients carry a reduced-form interpretation rather than structurally identified effects of inventories and transportation delays.

Our horizon-specific findings also show what a single scalar estimate of the spread–

cost relationship comprises. The exact finite-sample decomposition confirms that the conventional scalar coefficient is a combination of a variance-weighted within-band component and a cross-band covariance component, thereby quantifying how the estimate compresses distinct horizon-relevant heterogeneity into one scalar coefficient. In contrast, our proposed integration spectrum recovers the nuanced structure of the relationship between the spatial spread and transport cost by systematically distinguishing across short-, intermediate-, and long-run patterns. A battery of gain and phase diagnostics shows that the response gain rises from the transient to the trend horizon, even though it does not increase monotonically across the intermediate bands. This indicates that phase displacement between transport-cost variations and spatial spread adjustments alone does not fully explain the gain pattern, suggesting that the result is not merely an artifact of phase delay. Additionally, the coexistence of strong short-run basis comovement across the broader corn market and weak short-run transport-cost pass-through in the Illinois–Gulf corridor is consistent with a conceptual distinction between rapid cross-market price comovement and the slower adjustment of spatial price spreads to transport-cost variation.

Overall, the integration spectrum offers a practical measurement framework because it can be constructed from routinely reported weekly prices and route-specific transportation costs. By showing how the spread–cost relationship changes across horizons, the spectrum allows us to view market integration as a dynamic process that materializes over time rather than as a single static outcome. At the same time, the current application is deliberately limited in scope. It focuses on a single transport corridor and provides a reduced-form characterization of horizon dependence rather than separately identifying the economic mechanisms that generate it.

Our next steps in this study will be to investigate the mechanisms underlying the horizon gradient and assess the external validity of the results across additional markets and geographies. For the first extension, we aim to incorporate information regarding inventories and estimate Coleman-style regressions that account for destination inventory conditions and the time required for physical transportation. Second, we will include additional transport corridors, allowing us to assess whether the estimated horizon pattern generalizes beyond the Illinois–Gulf application and to examine corridor-specific freight costs within a broader spatial network. We also plan to extend the framework to other storable commodities. Finally, as longer and richer transportation-cost series become available, we will evaluate more flexible band structures rather than relying exclusively on pre-specified horizons.

References

Adjemian, M. K., Garcia, P., Irwin, S. H., & Smith, A. (2013). *Non-Convergence in Domestic Commodity Futures Markets: Causes, Consequences, and Remedies* (tech. rep. No. EIB-115). U.S. Department of Agriculture, Economic Research Service. https://doi.org/10.2139/ssrn.2323646

Balke, N. S., & Fomby, T. B. (1997). Threshold Cointegration. *International Economic Review*, *38*(3), 627–645. https://doi.org/10.2307/2527284

Barrett, C. B. (1996). Market Analysis Methods: Are Our Enriched Toolkits Well Suited to Enlivened Markets? *American Journal of Agricultural Economics*, *78*(3), 825–829. https://doi.org/10.2307/1243313

Barrett, C. B., & Li, J. R. (2002). Distinguishing between Equilibrium and Integration in Spatial Price Analysis. *American Journal of Agricultural Economics*, *84*(2), 292–307. https://doi.org/10.1111/1467-8276.00298

Baulch, B. (1997). Transfer Costs, Spatial Arbitrage, and Testing for Food Market Integration. *American Journal of Agricultural Economics*, *79*(2), 477–487. https://doi.org/10.2307/1244145

Baxter, M., & King, R. G. (1999). Measuring Business Cycles: Approximate Band-Pass Filters for Economic Time Series. *The Review of Economics and Statistics*, *81*(4), 575–593. https://doi.org/10.1162/003465399558454

Birge, J. R., Chan, T. C. Y., Pavlin, J. M., & Zhu, I. Y. (2022). Spatial Price Integration in Commodity Markets with Capacitated Transportation Networks. *Operations Research*, *70*(3), 1739–1761. https://doi.org/10.1287/opre.2022.2288

Brennan, M. J. (1958). The Supply of Storage. *American Economic Review*, *48*(1), 50–72.

Christiano, L. J., & Fitzgerald, T. J. (2003). The Band Pass Filter. *International Economic Review*, *44*(2), 435–465. https://doi.org/10.1111/1468-2354.t01-1-00076

Coleman, A. (2009). Storage, Slow Transport, and the Law of One Price: Theory with Evidence from Nineteenth-Century U.S. Corn Markets. *The Review of Economics and Statistics*, *91*(2), 332–350. https://doi.org/10.1162/rest.91.2.332

Deaton, A., & Laroque, G. (1992). On the Behaviour of Commodity Prices. *Review of Economic Studies*, *59*(1), 1–23. https://doi.org/10.2307/2297923

Engle, R. F. (1974). Band Spectrum Regression. *International Economic Review*, *15*(1), 1–11. https://doi.org/10.2307/2526084

Engle, R. F., & Granger, C. W. J. (1987). Co-integration and Error Correction: Representation, Estimation, and Testing. *Econometrica*, *55*(2), 251–276. https://doi.org/10.2307/1913236

Enke, S. (1951). Equilibrium among Spatially Separated Markets: Solution by Electric Analogue. *Econometrica*, *19*(1), 40–47. https://doi.org/10.2307/1907907

Fackler, P. L., & Goodwin, B. K. (2001). Spatial Price Analysis. In B. L. Gardner & G. C. Rausser (Eds.), *Handbook of agricultural economics* (pp. 971–1024, Vol. 1B). Elsevier.

Fackler, P. L., & Tastan, H. (2008). Estimating the Degree of Market Integration. *American Journal of Agricultural Economics*, *90*(1), 69–85. https://doi.org/10.1111/j.1467-8276.2007.01058.x

Fuller, W. A. (1987). *Measurement Error Models*. John Wiley & Sons. https://doi.org/10.1002/9780470316665

Garcia, P., Irwin, S. H., & Smith, A. (2015). Futures Market Failure? *American Journal of Agricultural Economics*, *97*(1), 40–64. https://doi.org/10.1093/ajae/aau067

Goodwin, B. K., Grennes, T. J., & Wohlgenant, M. K. (1990). A Revised Test of the Law of One Price Using Rational Price Expectations. *American Journal of Agricultural Economics*, *72*(3), 682–693. https://doi.org/10.2307/1243038

Goodwin, B. K., & Piggott, N. E. (2001). Spatial Market Integration in the Presence of Threshold Effects. *American Journal of Agricultural Economics*, *83*(2), 302–317. https://doi.org/10.1111/0002-9092.00157

Goodwin, B. K., & Schroeder, T. C. (1991). Cointegration Tests and Spatial Price Linkages in Regional Cattle Markets. *American Journal of Agricultural Economics*, *73*(2), 452–464. https://doi.org/10.2307/1242730

Goswami, A., Adjemian, M. K., & Karali, B. (2022). The impact of futures contract storage rate policy on convergence expectations in domestic commodity markets. *Food Policy*, *111*, 102301. https://doi.org/10.1016/j.foodpol.2022.102301

Granger, C. W. J. (1966). The Typical Spectral Shape of an Economic Variable. *Econometrica*, *34*(1), 150–161.

Granger, C. W. J., & Hatanaka, M. (1964). *Spectral Analysis of Economic Time Series*. Princeton University Press.

Johansen, S. (1988). Statistical Analysis of Cointegration Vectors. *Journal of Economic Dynamics and Control*, *12*(2–3), 231–254. https://doi.org/10.1016/0165-1889(88)90041-3

Kaldor, N. (1939). Speculation and Economic Stability. *The Review of Economic Studies*, *7*(1), 1–27. https://doi.org/10.2307/2967593

Künsch, H. R. (1989). The Jackknife and the Bootstrap for General Stationary Observations. *The Annals of Statistics*, *17*(3), 1217–1241. https://doi.org/10.1214/aos/1176347265

Lence, S. H., Moschini, G., & Santeramo, F. G. (2018). Threshold Cointegration and Spatial Price Transmission When Expectations Matter. *Agricultural Economics*, *49*(1), 25–39. https://doi.org/10.1111/agec.12393

McNew, K., & Fackler, P. L. (1997). Testing Market Equilibrium: Is Cointegration Informative? *Journal of Agricultural and Resource Economics*, *22*(2), 191–207. https://doi.org/10.22004/ag.econ.30853

Miljkovic, D., Price, G. K., Hauser, R. J., & Algozin, K. A. (2000). The Barge and Rail Freight Market for Export-Bound Grain Movement from Midwest to Mexican Gulf: An Econometric Analysis. *Transportation Research Part E: Logistics and Transportation Review*, *36*(2), 127–137. https://doi.org/10.1016/S1366-5545(99)00025-3

Müller, U. K., & Watson, M. W. (2008). Testing Models of Low-Frequency Variability. *Econometrica*, *76*(5), 979–1016. https://doi.org/10.3982/ECTA6814

Müller, U. K., & Watson, M. W. (2018). Long-Run Covariability. *Econometrica*, *86*(3), 775–804. https://doi.org/10.3982/ECTA15047

Myers, R. J., & Jayne, T. S. (2012). Multiple-Regime Spatial Price Transmission with an Application to Maize Markets in Southern Africa. *American Journal of Agricultural Economics*, *94*(1), 174–188. https://doi.org/10.1093/ajae/aar123

Nigatu, G., & Adjemian, M. K. (2020). A Wavelet Analysis of Price Integration in Major Agricultural Markets. *Journal of Agricultural and Applied Economics*, *52*(1), 117–134. https://doi.org/10.1017/aae.2019.35

Percival, D. B., & Walden, A. T. (2000). *Wavelet Methods for Time Series Analysis* (Vol. 4). Cambridge University Press.

Politis, D. N., & Romano, J. P. (1994). The Stationary Bootstrap. *Journal of the American Statistical Association*, *89*(428), 1303–1313. https://doi.org/10.1080/01621459.1994.10476870

Priestley, M. B. (1981). *Spectral Analysis and Time Series*. Academic Press.

Ravallion, M. (1986). Testing Market Integration. *American Journal of Agricultural Economics*, *68*(1), 102–109. https://doi.org/10.2307/1241654

Samuelson, P. A. (1952). Spatial Price Equilibrium and Linear Programming. *American Economic Review*, *42*(3), 283–303.

Scheinkman, J. A., & Schechtman, J. (1983). A Simple Competitive Model with Production and Storage. *The Review of Economic Studies*, *50*(3), 427–441. https://doi.org/10.2307/2297674

Sephton, P. S. (2003). Spatial Market Arbitrage and Threshold Cointegration. *American Journal of Agricultural Economics*, *85*(4), 1041–1046. https://doi.org/10.1111/1467-8276.00506

Stephens, E. C., Mabaya, E., von Cramon-Taubadel, S., & Barrett, C. B. (2012). Spatial Price Adjustment with and without Trade. *Oxford Bulletin of Economics and Statistics*, *74*(3), 453–469. https://doi.org/10.1111/j.1468-0084.2011.00651.x

Stigler, G. J., & Sherwin, R. A. (1985). The Extent of the Market. *Journal of Law and Economics*, *28*(3), 555–585. https://doi.org/10.1086/467101

Takayama, T., & Judge, G. G. (1971). *Spatial and Temporal Price and Allocation Models*. North-Holland.

Telser, L. G. (1958). Futures Trading and the Storage of Cotton and Wheat. *Journal of Political Economy*, *66*(3), 233–255. https://doi.org/10.1086/258036

U.S. Department of Agriculture, Agricultural Marketing Service. (2026a). *Downbound Grain Barge Rates* [Agricultural Transportation Open Data Platform (AgTransport)]. Retrieved August 1, 2026, from https://agtransport.usda.gov/Barge/Downbound-Grain-Barge-Rates/deqi-uken

U.S. Department of Agriculture, Agricultural Marketing Service. (2026b). *Grain Basis* [Agricultural Transportation Open Data Platform (AgTransport)]. Retrieved August 1, 2026, from https://agtransport.usda.gov/Grain/Grain-Basis/v85y-3hep

U.S. Department of Agriculture, Agricultural Marketing Service. (2026c). *Grain Price Spreads* [Agricultural Transportation Open Data Platform (AgTransport)]. Retrieved August 1, 2026, from https://agtransport.usda.gov/Grain/Grain-Price-Spreads/an4w-mnp7

U.S. Department of Agriculture, Agricultural Marketing Service. (2026d). *Historical U.S. Rail Tariff Rates for Grain and Soybeans* [Agricultural Transportation Open Data Platform (AgTransport)]. Retrieved August 1, 2026, from https://agtransport.usda.gov/Rail/Historical-U-S-Rail-Tariff-Rates-for-Grain-and-Soy/idbx-qf4w

U.S. Department of Agriculture, Agricultural Marketing Service. (2026e). *Secondary Railcar Auction Market Bids* [Agricultural Transportation Open Data Platform (AgTransport); enters the rail cost of the min(barge, rail) robustness series]. Retrieved August 1, 2026, from https://agtransport.usda.gov/Rail/Secondary-Railcar-Auction-Market-Bids/cvu8-kpyk

Vetterli, M., & Herley, C. (1992). Wavelets and Filter Banks: Theory and Design. *IEEE Transactions on Signal Processing*, *40*(9), 2207–2232. https://doi.org/10.1109/78.157221

von Cramon-Taubadel, S., & Goodwin, B. K. (2021). Price Transmission in Agricultural Markets. *Annual Review of Resource Economics*, *13*, 65–84. https://doi.org/10.1146/annurev-resource-100518-093938

Whitcher, B., Guttorp, P., & Percival, D. B. (2000). Wavelet Analysis of Covariance with Application to Atmospheric Time Series. *Journal of Geophysical Research: Atmospheres*, *105*(D11), 14941–14962. https://doi.org/10.1029/2000JD900110

Williams, J. C., & Wright, B. D. (1991). *Storage and Commodity Markets*. Cambridge University Press.

Working, H. (1948). Theory of the Inverse Carrying Charge in Futures Markets. *Journal of Farm Economics*, *30*(1), 1–28. https://doi.org/10.2307/1232678

Working, H. (1949). The Theory of Price of Storage. *American Economic Review*, *39*(6), 1254–1262.

A Supplementary Appendix

Table A.1: Conventional summaries versus band coherence, two simulated market sets.

summary statistic	set 1 (transmitted)	set 2 (local noise)
Johansen cointegrating coefficient	0.994	1.001
VECM adjustment speed (EC loading)	-0.106	-0.073
IRF half-life (weeks)	4.167	4.333
threshold regime split	0.819	0.663
rolling cointegration frequency	0.972	0.939
transient-band coherence	0.798	0.005
varying-cost trend coefficient (truth 1)	1.011	0.971
varying-cost transient coefficient (truth 1)	0.805	1.045
varying-cost transient R-squared	0.013	0.018

Notes: Two simulated market sets. The long-run and univariate summaries nearly coincide (Johansen β (Johansen, 1988) 0.994 vs 1.001; IRF half-life 4.2 vs 4.3 weeks; rolling cointegration 0.97 vs 0.94); the threshold regime split and the VECM loading move (0.819 vs 0.663; -0.106 vs -0.073) but carry no transmission verdict. Only the transient-band coherence separates the sets (0.798 vs 0.005). The final three rows are a companion varying-cost recovery design (band β against a truth of one; the transient R^2 is small by construction).

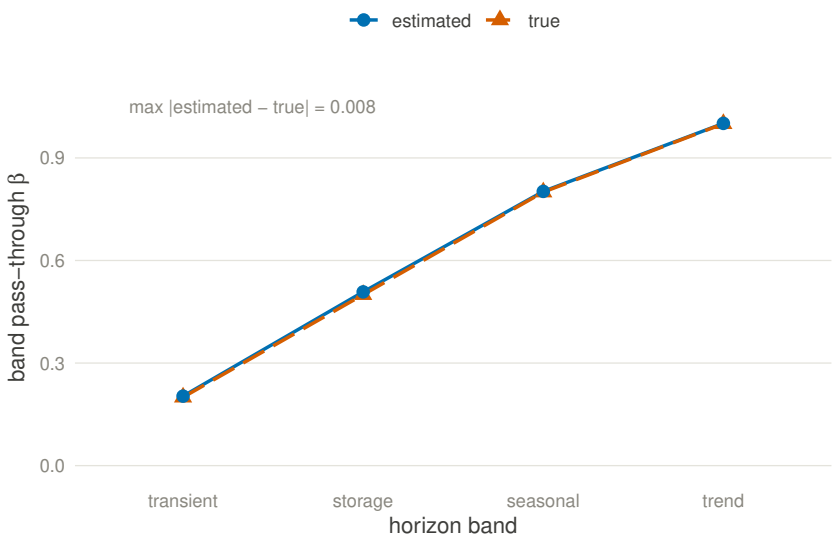


Figure A.1: Known-spectrum recovery on a rising-β DGP, under the same finite-filter procedure used on the data.

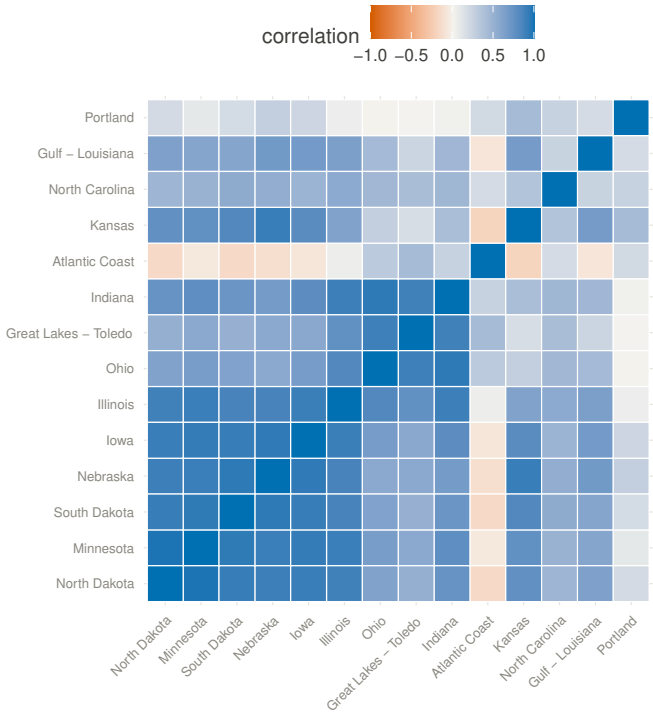


Figure A.2: Cross-market weekly-basis correlation.